

**C. Déprés**  
(SYMME)  
**C. Robertson**  
(SRMA, CEA )  
**M. Fivel**  
(SIMaP, CNRS)

E-mail: Marc.Fivel@simap.grenoble-inp.fr

DOI : 10.12762/2015.AL09-01

# 3D Discrete Dislocation Dynamics Investigations of Fatigue Crack Initiation and Propagation

**B**oth nucleation and propagation of fatigue cracks in fcc metals are investigated, using 3D discrete dislocation dynamics (DDD) simulations. Firstly, DDD simulations explain the mechanisms leading to the formation of persistent slip bands in surface grains loaded in fatigue. Extrusions are evidenced where the bands intercept the free surface. The extrusion growth rate is estimated for different material parameters and loading conditions. Energy and stress calculations performed inside the simulated grain lead to a possible scenario for the crack initiation at the interface between the band and the matrix, as reported in the literature. Secondly, a crack is inserted at the persistent slip band interface and the crack tip slip displacement evolutions are evaluated. It is shown that the crack growth rate is strongly related to the grain size and to the distance to the grain boundary; the smaller the grain, the faster the crack growth. Finally, the crack propagation to the next grain is investigated by conducting DDD fatigue simulations in a surface grain next to a cracked grain. It is shown that the development of the persistent slip band is modified by the presence of the crack. The crack orientation affects the orientation of the persistent slip band, as well as the extrusion rate, and consequently the crack propagation in the next grain.

## Introduction

In single phased fcc materials, such as Copper or 316L stainless steels, stage-I fatigue cracks initiate in surface grains and the crack location is strongly correlated to the extrusion relief associated with the development of persistent slip bands [1, 10, 14, 15]. After the initiation stage, micro-cracks grow and cut the primary grain up to a first micro-structural barrier (a grain boundary, for example). At this point, subsequent propagation can be delayed for a certain time, depending on the loading amplitude and the orientation of the next grain [4]. Under high cycle fatigue (HCF) conditions, plasticity developing ahead of the first micro-structural barrier is a crucial and yet poorly understood phenomenon, possibly controlling the fatigue lifetime [2, 11, 13, 23].

Our goal in this work is to revisit the literature data on fatigue crack initiation and propagation in the low strain regime [19], using 3D discrete dislocation dynamics simulations. This numerical tool has the unique capacity to relate the organization of the dislocation lines to the mechanical properties of the material using very few model parameters.

## Simulation setup

All of the DDD simulations presented here use the edge-screw model TRIDIS developed by Verdier et al. [21]. The simulation box consists of a polygonal grain, typically a truncated dodecahedron or a faceted cylinder (figure 1). All surfaces are impermeable to dislocation motion, except for one free surface from which dislocations can escape, leaving a step. The image forces are not accounted for, since their effect was shown to be negligible [6]. The evaluation of the dislocation displacement at the surface is computed using a dedicated algorithm proposed in [12]. The loading conditions correspond to a uniaxial tension applied along the direction [-123]. The fatigue load is applied in a quasi-static manner. The stress is incremented when the dislocations have all reached a stable position. The stress rate is reversed when the cumulated plastic strain reaches the desired strain amplitude (typically  $10^{-3}$ ). The initial configuration for the dislocations consists of a single Frank-Read source located in the center of the simulation box. It was demonstrated that such a simple configuration was sufficient to develop the expected fatigue microstructure.

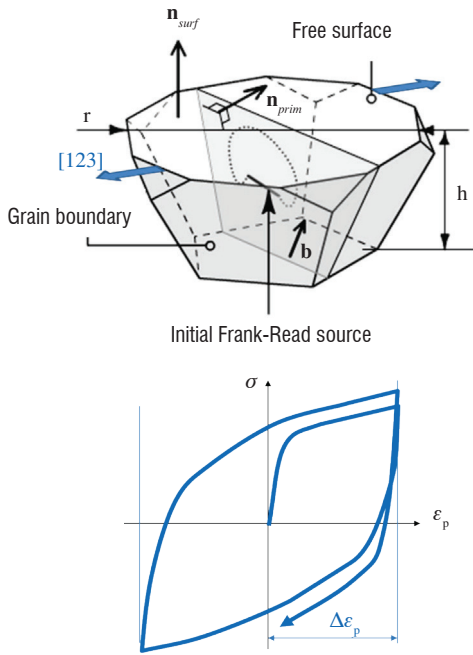


Figure 1 - DDD configuration and applied loading for the fatigue simulations of surface grains

Experimental observations of persistent slip bands developed in 316L stainless steels loaded in fatigue yielded the typical orientations of the simulation box. Typically, the normal to the free surface is fixed at  $\mathbf{n}_{surf} = (221)$  and the primary slip system for the Frank-Read source is  $a/2[110](1-1-1)$ .

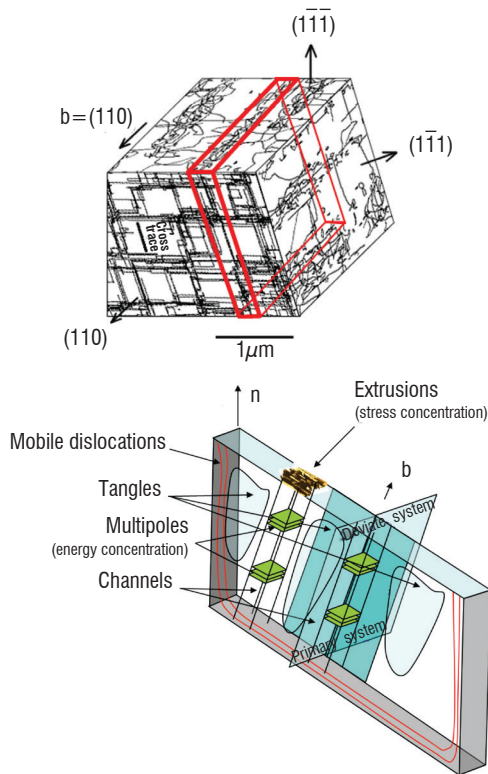


Figure 2 - Typical 3D dislocation microstructure and description of a single slip band [7]

## Persistent slip band formation

When the load is applied, the dislocation source quickly activates and emits dislocation loops in the simulated volume. Then, numerous cross slip events take place that spread the dislocation lines on the two associated slip systems: the primary slip system  $a/2 [110] (1-1-1)$  and the deviate slip system  $a/2 [110] (1-11)$ . This tends to homogenize the dislocation density and consequently the plasticity in the entire grain, which is beneficial to the fatigue life of the material. After a few cycles however, cross slip events and line reconnections modify the dislocation microstructure, which now becomes localized in bands [7].

A close look at a typical slip band shows that the band is made of channels, multipoles, tangles and mobile dislocations, as depicted in figure 2b. The multipoles consist of dipolar prismatic loops that can glide in the channels. The tangled dislocations are located near the channels, where dislocations hardly move.

## Extrusion growth mechanisms

The plastic steps imprinted on the surface by the escaping dislocations are calculated in the vicinity of the persistent slip bands. It is shown that an extrusion progressively develops at the intersection of the channels and the free surface [8]. Note that the surface relief consists mainly of extrusions (figure 3a), with very few intrusions in good agreement with experimental observation [10]. Interestingly, the predominance of extrusion compared to intrusions is obtained here using purely conservative dislocation motion and dislocation reactions, since in the DD model, dislocation climb and point defect diffusion are not taken into account.

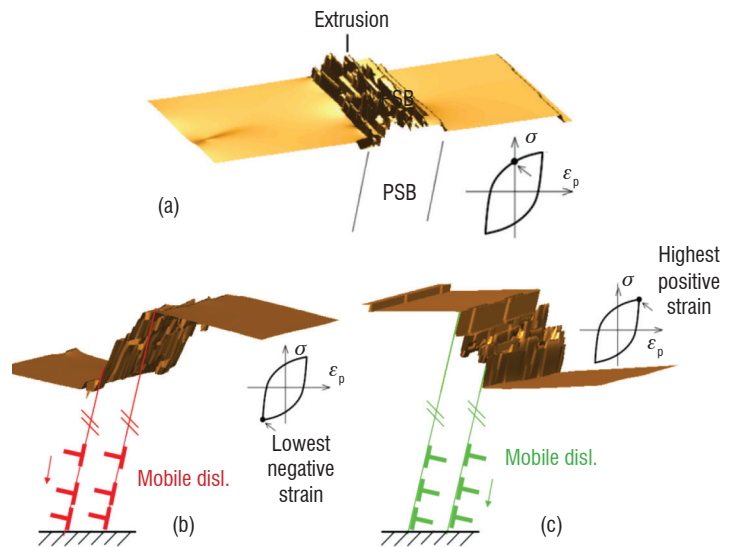


Figure 3 - Extrusion at the surface plotted for different instant of a given cycle

In figures 3b and 3c, the same surface zone is plotted when the plastic strain is maximum, negative and positive, respectively. The surface profile shows that most of the deformation is accommodated by two slip planes located at the interface between the band and the matrix. This demonstrates that these two planes contain highly mobile dislocations that can easily propagate in any of the two directions, depending on the sign of the applied stress. These mobile dislocations play a key role in the extrusion mechanism, since they

generate stress gradients that can sweep the multipoles located in the channels. The multipoles then reach the surface and create the extrusions, as shown in figure 3. The fact that on average the number of intrusions is lower than the number of extrusions means that most of the multipoles are made of interstitial prismatic loops. More work needs to be done to explain why vacancy prismatic loops are not swept toward the surface, but one should bear in mind that the DDD model is fully conservative, so that the dislocation microstructure contained in the grain is geometrically equivalent to the set of vacancy loops needed to exactly compensate the extrusions forming at the surface.

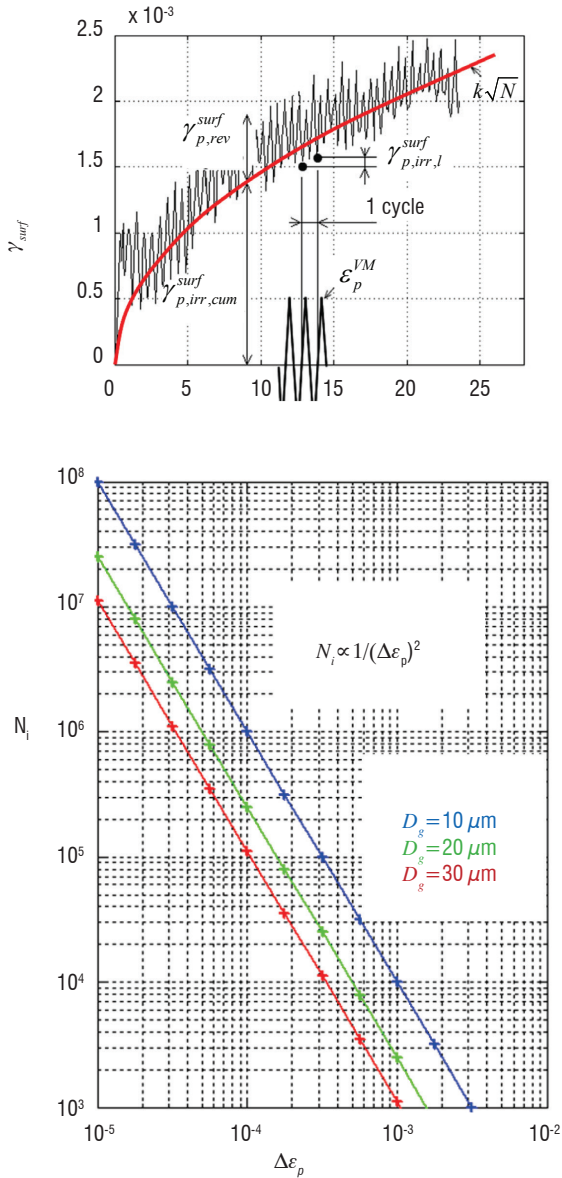


Figure 4 - Evolution of the irreversibility defined as the surface shear  $\gamma_{surf}$  and number of cycles needed to obtain a critical value of  $\gamma_{surf}$

In order to quantify the irreversibility cumulated with the cycles, we have defined the surface shear  $\gamma_{surf}$  as the total length per unit area of the plastic steps left on the free surface and projected along the surface normal vector  $\mathbf{n}_{surf}$ . A typical curve of  $\gamma_{surf}$  versus the number of cycles is given in figure 4. Although some part of  $\gamma_{surf}$  is recovered during a given cycle, the curves can be nicely fitted using a square root relationship, with the number of cycles demonstrating

a monotonic increase of the irreversibility. This means that the extrusion amplitude is continuously increasing, based on plasticity mechanisms.

A parametric study was conducted in order to measure the effect of the strain amplitude  $\Delta\epsilon_p$ , the mean strain  $\epsilon$ , the grain height  $h_g$  and the grain diameter  $D_g$ . It is found that the surface shear can be fitted by equation (1) below.

$$\gamma_{surf}(N) = K \frac{h_g}{D_g} \Delta\epsilon_p \left( 1 + 2 \frac{|\bar{\epsilon}|}{\Delta\epsilon_p} \right) \sqrt{N} \quad (1)$$

According to various authors, a critical value could be defined for the surface shear (or the extrusion height) that could initiate a crack [5, 17]. Figure 4 shows the number of cycles,  $N_i$ , required to reach a critical value of the cumulated shear  $\gamma_{surf}$  as a function of the strain amplitude and for different grain diameters. The power law scales with  $\Delta\epsilon^{-2}$ .

### Crack initiation scenario

In order to check where and when the first crack would most probably initiate, we have calculated the evolutions of the stresses and energies developed inside the slip bands. Figure 5a shows the typical distributions of the stored elastic energies at cycles number 5 and 19. Figure 5b shows the evolution of the maximum energy, evaluated as the standard deviation of the distribution. One can see that the maximum energy increases with the number of cycles. Assuming that such behavior could be extrapolated to a larger number of cycles, this means that after a given number of cycles a sufficient amount of elastic energy will be stored in the volume, which could lead to the formation of a crack. However, the crack will nucleate only if in the same region the stress tensor is able to promote atomic de-cohesions of the (111) planes. This effect can be evaluated using the same statistical analysis on the stress components (namely the shear and normal components), as plotted in figures 5c and 5d. The DD simulations show that the shear component (figure 5c) increases with the number of cycles, which is explained by the densification of the multipoles in the channels. However, the normal stress component, plotted in figure 5d, quickly saturates after a few cycles. Consequently, there will never be sufficient stress to be able to open a crack within the slip bands. Such a component is however present at the surface, where the extrusion shape concentrates the applied loading. Since the extrusion height is always increasing, the stress concentration also continuously increases up to the critical stress needed for atomic de-cohesions.

Finally, a complete crack initiation scenario could be drawn from the DD simulations (figure 6). The first crack will be nucleated for a given value of the irreversibility indicator,  $\gamma_{surf}$ , i.e., a given extrusion height, when a set of multipoles swept by the mobile dislocations will reach the surface, causing the strain energy to be sufficient at this location to open the crack. In practice, the de-cohesion stress needed to open the crack is reduced by the contaminations of the fresh surface steps developed with the cycles.

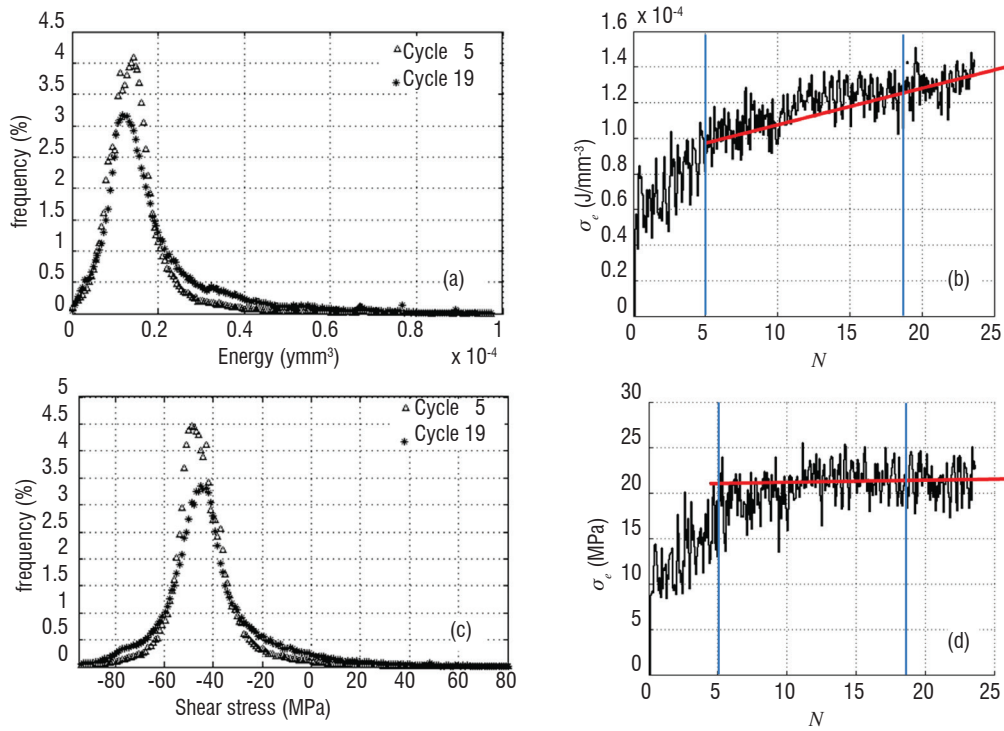


Figure 5 - Statistic analysis of the strain energy (a) and the stress components (c) and corresponding evolutions of the maximum strain energy (b) and the normal stress (d)

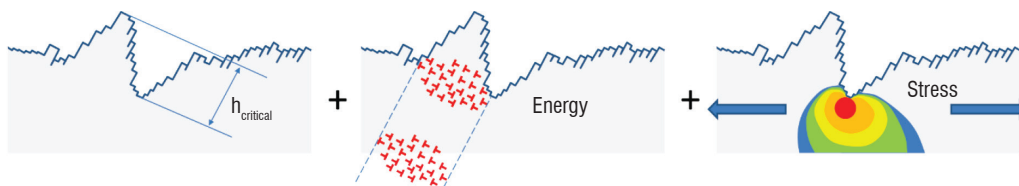


Figure 6 - Schematic description of the crack initiation scenario. The threshold condition is reached when the elastic energy (associated to the multipoles) and the stress concentration (related to the extrusion shape) coincide

## Crack propagation in the first grain

According to the crack initiation scenario presented in the previous section, the first crack should nucleate at the interface between the slip band and the matrix. In this section we will artificially insert a crack at this location by modifying the DD code in three manners [9].

(i) The two free surfaces corresponding to the crack lips are introduced in the simulated volume. The opening angle of the crack is fixed at  $10^{-2}$  radians. Similarly to the top free surface, the dislocations are allowed to cross the crack surfaces and to imprint plastic steps simulating the blunting process. Note that in this study, the image forces induced by the free surfaces are not accounted for, since their effect on the crack propagation was demonstrated to be limited in [7].

(ii) The crack stress field is introduced as Irwin's singular analytical expression for a 2D infinite crack [19] p.289. For each dislocation segment, the crack stress field is superimposed to the local effective stress.

(iii) Additional dislocation sources (one per slip system) are randomly inserted ahead of the crack tip, in order to account for crack tip plasticity.

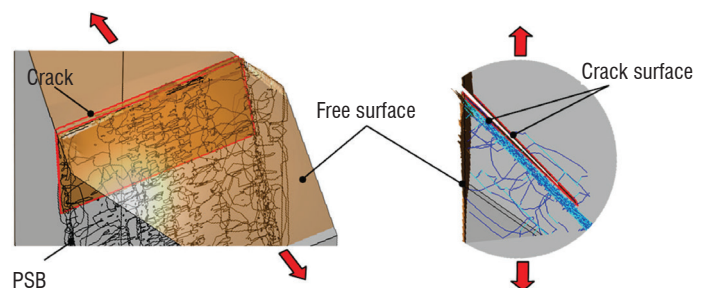


Figure 7 - Insertion of a crack in the 3D DD simulations

Figure 8 shows the dislocation microstructure and the evolution of the dislocation densities on the twelve slip systems in the case of a grain of diameter 10 microns. It is observed that the dislocation microstructure is not drastically modified by the insertion of crack.

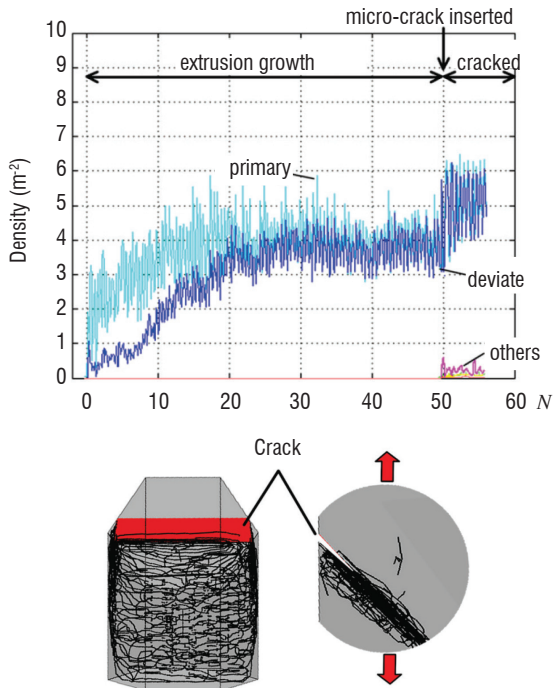


Figure 8 - Evolution of the dislocation densities and corresponding final dislocation microstructure developed in the cracked grain. The crack is inserted at cycle number 50

This is confirmed by the dislocation density accumulation rate, which remains similar after the crack insertion. It is also found that the crack shape remains sharp with highly reversible slip at the tip. Complementary simulations were performed in the case of a grain for which the crack was inserted from the beginning of the simulation, i.e., without a prior persistent slip band dislocation structure [9]. In this case, the dislocation microstructure is not planar anymore at the crack tip and the dislocation densities are more dispersed on the twelve possible slip systems, leading to crack tip blunting. This demonstrates that the slip band microstructure facilitates crack propagation through the first grain.

The crack propagation mechanism is also affected by the grain boundary. When the crack becomes close to the grain boundary, it is no longer possible to accommodate the plasticity ahead of the tip using only the primary and deviate slip systems. Consequently, the dislocation microstructure spreads on all of the slip systems, resulting in strong blunting effects, as shown in figure 9.

The effect of the distance to the grain boundary depends on the grain size,  $D_g$ . The slip dispersion is less pronounced in smaller grains. The consequence for small grains is that plasticity is more localized, so the crack propagation is faster. Such a feature is confirmed experimentally [20]. This effect is now quantified by computing the Crack Tip Slip Displacement ( $CTSD$ ) for different distances to the grain boundary and for different grain sizes, the grain shape ratio being conserved. The  $CTSD$  is calculated by averaging displacement profiles taken along 100 lines crossing the crack tip. Results are given in figure 10. The ratio  $CTSD/D_g$  is found to be almost independent from the grain size for crack lengths smaller than 50% of the grain size. In other words, the

$CTSD$  is proportional to the grain size, so the number of cycles needed for the crack to move over half the grain is more or less the same, regardless of the grain size. For a greater crack length, i.e., for a crack closer to the grain boundary, the  $CTSD$  is strongly reduced for larger grains, indicating that crack propagation is slower in coarser grains, as reported in [19] and [3].

The curves in figure 10a can be nicely fitted using equation (2) below [9],

$$\frac{CTSD}{D_g} \cong \Delta \varepsilon_p \left( 1 - \exp \left( - \frac{\lambda}{\Delta \varepsilon_p} \frac{b}{D_g} \left( 1 - \frac{a}{D_g} \right) \right) \right) \quad (2)$$

where  $a$  is the crack length and  $\lambda=25$  is a fitting parameter.

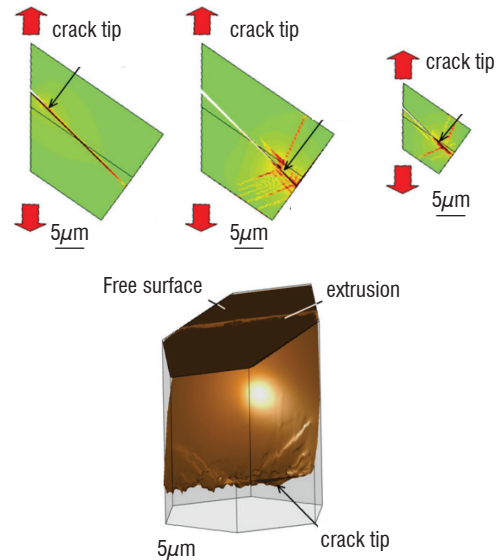


Figure 9 - Effect of the distance to the grain boundary. Dispersed plastic slip and crack tip blunting is observed for the shortest distances

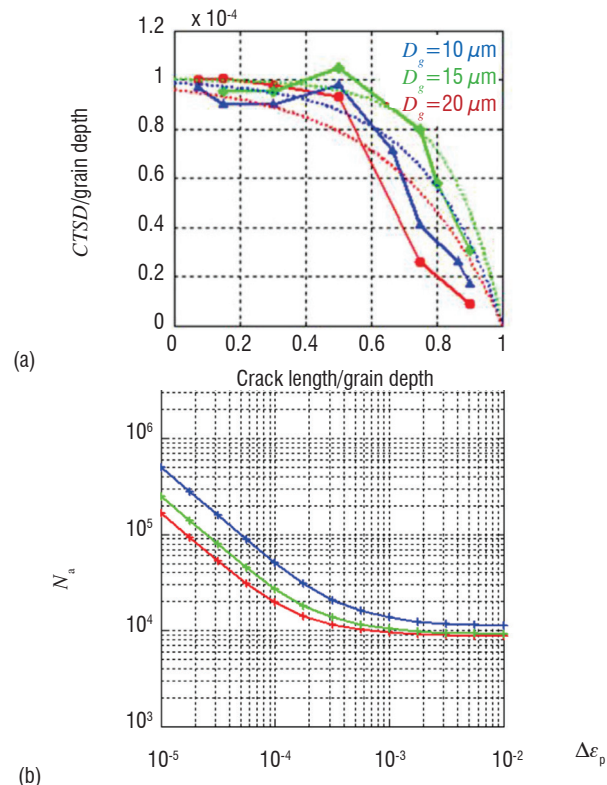


Figure 10 - Crack Tip Slip Displacement versus the distance between the crack and the grain boundary for different grain sizes and numbers of cycles to obtain a 5 micrometer length crack using equation (1)

Assuming that the crack propagates over a distance  $CTSD$  every  $N_i$  cycles, we can integrate Equation (2) in order to estimate the number of cycles required for a crack to propagate over a given length. Figure 10b shows the curves corresponding to a crack propagation of  $a=5\ \mu m$  for different grain sizes. For low plastic strain amplitudes, the number of cycles is found to be proportional to  $\Delta\varepsilon_p^{-1}$ , whereas for higher strain amplitudes the number is almost constant. Note also that this number is very low compared to the number of cycles needed for crack initiation, which is proportional to  $\Delta\varepsilon_p^{-2}$  as shown by Equation (1) and plotted in figure 4. This shows that crack initiation takes much longer than crack propagation.

### Crack propagation towards the next grain

Focusing on the crack propagation in surface grains, the objective of this section is to investigate the crack interaction with the first microstructural barrier. The study of the crack propagation in the first grain showed that most of the plasticity at the crack tip was accommodated by the Burgers vector of the primary/deviate slip systems forming the persistent slip band. Such a Burgers vector is almost perpendicular to the free surface (figure 1) and, consequently, coplanar with the grain boundary. Thus, the scenario for the crack transmission mechanism from one grain to the next grain is more likely to be an 'indirect transmission', as depicted in figure 11. This means that the cracks will not be able to shear and cross the grain boundary, but will rather generate a new slip band in the next grain, which will later initiate a crack in the same way as in the first grain.

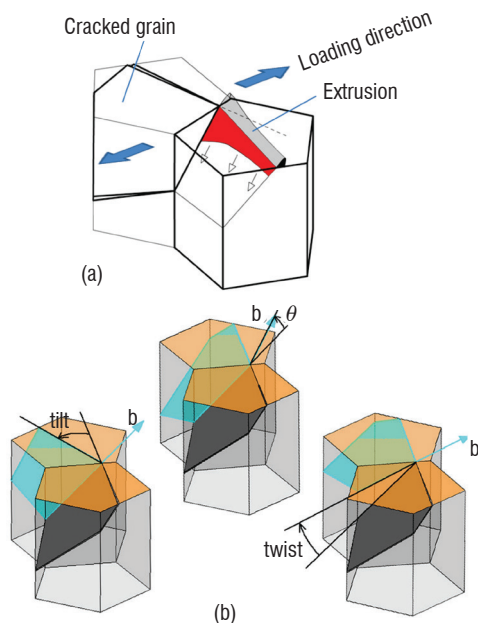


Figure 11 - Simulation setup.  
 (a) Indirect transmission mechanism  
 (b) Definition of the three relative angles defining the relative position of the crack with respect to the slip band

The simulation setup consists of a cracked grain, for which the crack is once again represented by the singular stress field of a 2D infinite crack. The next grain corresponds to the DD simulation box. The initial dislocation microstructure includes 24 Frank-Read sources, randomly distributed in the simulated grain on all of the possible slip systems. The fatigue load is imposed with a plastic strain amplitude of  $\Delta\varepsilon_p = 10^{-4}$

relevant to High Cycle Fatigue (HCF) conditions. The crack orientation is defined by the tilt, twist and theta angles between the crack and the slip band planes.

A typical result is shown in figure 12. The curve marked as (a) shows the surface shear accumulated in the grain before the crack is inserted. The corresponding dislocation microstructure obtained after a few cycles is given in the same figure. The formation of a slip band can be clearly seen. The crack is inserted at cycle number 34 and the surface shear is modified into curve (b), which shows a larger accumulation rate of the surface shear. The corresponding dislocation microstructure obtained after a few more cycles shows that the slip band has been destroyed and a new one has formed on a different set of slip systems.

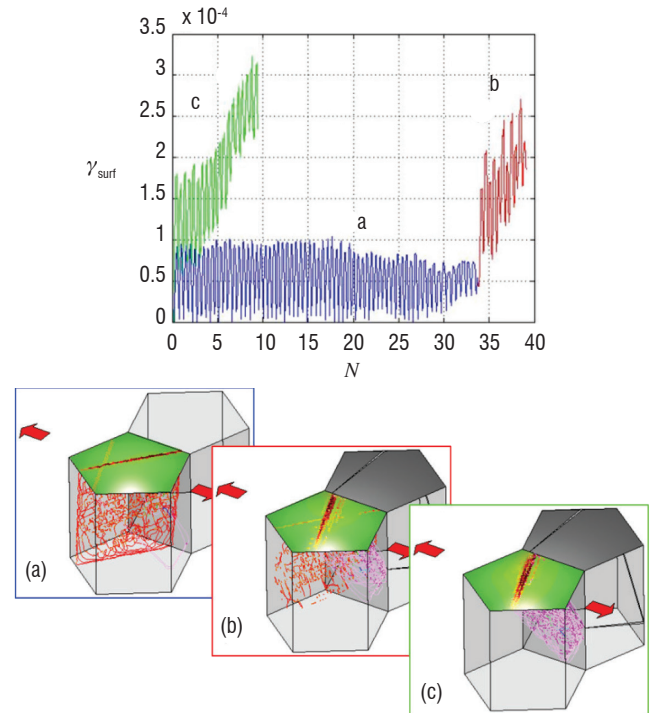


Figure 12 - Effect of the crack on the irreversibility  
 (a) The crack has not yet been introduced  
 (b) The crack is introduced, after 34 fatigue cycles  
 (c) The crack has been introduced as from the beginning

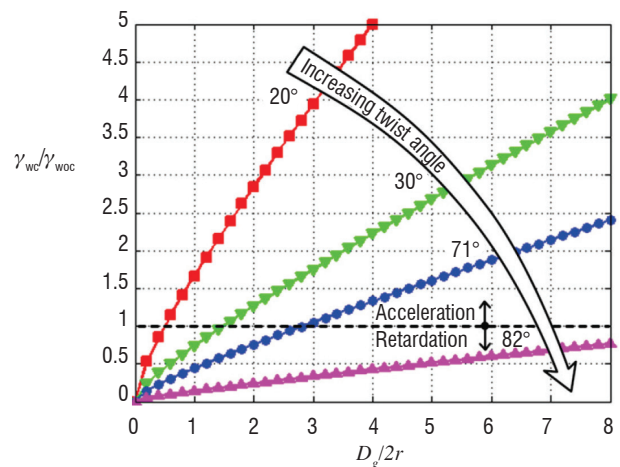


Fig. 13 - Ratio of the surface shear in the presence of the crack / surface shear without any crack for a tilt angle of  $24^\circ$  and for different twist angles

If the crack is introduced from the beginning of the fatigue simulation, it gives the surface shear and dislocation microstructure indicated as (c) in figure 12. Both are similar to sequence (b) obtained when the crack was inserted after a few cycles. This means that the crack imposes both its own dislocation microstructure and its own extrusion rate. In other words, the dislocation microstructure formed in the grain could not have been predicted from Schmid's law predictions, as used in continuum models.

A parametric study was conducted by varying the twist and tilt angles [16]. It is found that in some cases the crack insertion can speed up the accumulation rate and for other situations it can slow down the extrusion growth. This is illustrated in figure 13, where the surface shear accumulated in the grain has been divided by the reference surface shear accumulated in a grain without any crack. If the ratio is greater than 1, the crack increases the extrusion growing rate, whereas a value below 1 is the signature of a delaying effect of the crack on the extrusion growth rate. The curves are plotted as a function of the distance to the crack tip,  $r$ .

## Concluding remarks

3D DD simulations helped in understanding persistent slip band formation and the associated surface extrusion growth mechanisms. A detailed scenario for the crack initiation is proposed, where the mechanism for the crack propagation along the slip band is explained and quantified as a function of the grain size. Finally, the crack transmission to the next grain is investigated for diverse crack orientations, showing that the crack plays a major role in the development of plasticity in the neighboring grains.

Despite the promising results obtained in this study, the DD simulations conducted here have several limitations. The first one is related to the calculation time required for a simulation, which limits the maximum number of simulated cycles. Moreover, neither the surface contamination, nor diffusion mechanisms are taken into account in the model. Finally, the DDD simulations were all performed in a single crystal. The perspectives of this work consist in overcoming these limitations by improving the model, both in terms of the physics and computational efficiency ■

## Acknowledgements

The funding of this research through CPR-SMIRN as well as ANR AFGRAP is gratefully acknowledged.

## References

- [1] Z.S. BASINSKI, S.J. BASINSKI - Prog. Mater. Sci., Vol. 36, 1992.
- [2] TR BIELER, P. EISENLOHR, F. ROTERS, D. KUMAR, D.E. MASON, M.A. CRIMP, D. RAABE - Int J of Plast, Vol. 25, 2009.
- [3] C. BLANKENSHIP, E. STARKE - Fat. Frac. Eng. Mat. Str., Vol. 14, 1991.
- [4] H.J. CHRIST, O. DUBER, C.P. FRITZEN, H. KNOBBE, P. KÖSTER, U. KRUPP, B. KÜNKLE - Comput Mater Sci Vol. 46, 2009.
- [5] L. CRETEGNY AND A. SAXENA - Acta Mater. Vol. 49, No. 18, 2001.
- [6] C. DÉPRÉS - Ph.D. Thesis, Grenoble INP, 2004. (download from <http://www.numodis.fr/tridis>)
- [7] C. DÉPRÉS, C.F. ROBERTSON, M.C. FIVEL - Phil. Mag., Vol. 84, No. 22, 2004.
- [8] C. DÉPRÉS, C.F. ROBERTSON, M.C. FIVEL - Phil. Mag., Vol. 86, No. 1, 2006.
- [9] C. DÉPRÉS, V.G. PRASAD REDDY, C.F. ROBERTSON, M.C. FIVEL - Phil. Mag., Vol. 94, No.36, 2014.
- [10] U. ESSMANN, U. GÖSELE, H. MUGHRABI - Phil. Mag. A, Vol. 44, No. 2, 1981.
- [11] E. FERRIÉ M. SAUZAY - J. Nucl Mater, Vol. 386-388, 2009.
- [12] M. FIVEL AND C. DÉPRÉS - Phil. Mag., Vol. 94, No. 28, 2014.
- [13] Y. HONG, Y. QIAO, N. LIU, X. ZHENG - Fat. Fract Eng Mater Struct, Vol 21, 1998.
- [14] J. MAN, K. OBRTLİK, C. BLOCHWITZ, J. POLAK - Acta Mater. Vol. 50, 2002.
- [15] J. MAN, K. OBRTLİK, J. POLAK - Phil. Mag. A, Vol. 89, No. 16, 2009.
- [16] V.G. PRASAD REDDY, C.F. ROBERTSON, C. DÉPRÉS, M.C. FIVEL - Acta Mater., Vol. 61, 2013.
- [17] M. RISBET, X. FEAUGAS, C. GUILLEMER-NEEL, M. CLAVEL - Scripta Mat. Vol. 49, 2003.
- [18] C.S. SHIN, C.F. ROBERTSON, M.C. FIVEL - Phil. Mag., Vol. 87, No. 24, 2007.
- [19] S. SURESH - *Fatigue of Materials*. Cambridge University Press, Cambridge, 1998.
- [20] A. VAN DER VEN, G. CEDER - Acta Mater, Vol. 52, 2004.
- [21] M. VERDIER, M. FIVEL, I. GROMA - *Modelling Simul. Mater. Sci. Eng.*, Vol. 6, No.6, 1998.
- [22] Y. QIAO, S.S. CHAKRAVARTHULA - Int J Fatigue 2005, Vol. 27, 1251.
- [23] Y. QIAO - Mate. Sci Eng 2003, Vol. A361:350.

## AUTHORS

---



**Christophe Déprés** graduated from the Ecole Normale Supérieure de Cachan, France and obtained a Ph.D. in Mechanics from the Grenoble Institute of Technology in 2004. He is now an assistant professor at the Laboratoire SYMME, Université Savoie Mont Blanc. His research field focuses on plasticity problems, such as fatigue or dislocation based model development, taking advantage of the potential of Discrete Dislocation Dynamics simulations.



**Christian Robertson** graduated from the Ecole Polytechnique de Montréal (Canada) in 1995 with a Masters Degree in Physical Engineering and then, in 1998, achieved a Doctoral Degree from the Université de Paris 6 (France), in Materials Science. In 2000, he started his career at CEA, the French Atomic Energy Commission (Nuclear Materials Department), as a research engineer. He became an expert in micro-plasticity mechanisms in metallic materials under extreme conditions (high temperature, high radiation dose, fatigue, etc.). His research activity combines microscopic observations and numerical simulations.



**Marc Fivel** graduated from the Ecole Normale Supérieure de Cachan, France and obtained a Ph.D. in Mechanics from the Grenoble Institute of Technology in 1997. After a post-doctoral position at Lawrence Livermore National Laboratory (USA), he was hired at CNRS in 1998. He is now a CNRS Research Professor at SIMaP-GPM2, University Grenoble Alpes. His areas of interest include multiscale simulations of crystal plasticity with a special focus on discrete dislocation dynamics simulations.